International Research Journal of Engineering and Technology (IRJET) e-ISSN: 2395-0056
Volume: 09 Issue: 05 | May 2022 www.irjet.net p-ISSN: 2395-0072

DESIGN OF SLOTTED WAVEGUIDE ANTENNA FOR WIRELESS APPLICATION

[*1] Mr. Monish Raj. D, [*2]Dr. Rajesh Kumar. V

*[*1]M.Tech Student, School of Electronic Engineering (Sense), Vellore Institutions of Technology, Vellore*
*[*2]Professor, School of Electronic Engineering (Sense), Vellore Institutions of Technology, Vellore*

Abstract- Slotted waveguide antenna (SWA) arrays have different advantages in terms of design, weight, volume, power handling, directivity, and efficiency. For broadwall SWAs, the slot displacements from the wall centerline determine the antenna's side lobe level (SLL). It demonstrates how to use a simple novel approach to create broad wall SWAs with acceptable SLLs. Given the needed SLL and operating frequency, this algorithm discovers the slots length, width, locations along the length of the waveguide, and displacements from the centerline for a given number of identical longitudinal slots. Because all slots have the same length and the displacements are calculated using closed-form equations, this approach is much easier than prior methods. A computer programme was designed to do the design calculations and generate the needed slots data. The Taylor, Chebyshev, and binomial distributions are all used in instances. In these cases, elliptical slots are employed because their rounded corners make them more resistant in high-power applications. The results of prototyping and testing a SWA are consistent with the design goals..

Keywords: SWA Antenna, SLL, E-Plane, H-Plane, Bandwidth, Displacement and co-efficiency, microwave application

1. INTRODUCTION

Rectangular Slotted Waveguide Antennas (SWAs) transmit radiation through slots carved in the broad or thin wall of a rectangular waveguide. As a result, the radiating elements are integrated into the waveguide's feed system, resulting in a simplified design that does not require balloons or matching networks [5].SWAs also have a low weight and small volume, as well as a high power handling capacity, high efficiency, and an excellent reflection coefficient. They've been perfect for numerous radar, communications, navigation, and high-power microwave applications because of this. Depending on how the wave propagates inside the waveguide, SWAs can be resonant or non-resonant., The former is a standing wave, whereas the later is a travelling wave [6]. Although the traveling-wave SWA has a higher bandwidth, it requires a matching terminating load to absorb the wave and prevent it from being reflected, reducing its efficiency. It also has the drawback of the main beam direction being dependent on the operating frequency. The end of the waveguide in resonant SWAs is terminated with a short circuit, resulting in improved efficiency due to no power loss at the waveguide end. Furthermore, regardless of frequency, the primary beam is normal to the array, although these benefits come at the cost of a restricted operation band [3].

2. Background

It demonstrated a planar SWA at 140 GHz. The feeder SWA, which consists of a feeding slot, an overrode cavity, and coupling slots, was developed to provide excitations of the same amplitude but in alternating phases. An integrated power divider and phase shifter were used to accomplish this [4]. Coupling was also done using longitudinal slots with the same lengths and offsets. Kumar et al22 proposed using a planar SWA in the X-band. The desired current distribution was synthesised using a genetic algorithm paired with Schelkunoff's unit circle approach. The inclined coupling slot layer and a feed layer with a power divider were the two layers that made up the feeder. Zhang et al.23 have demonstrated a planar SWA that operates at 40 GHz. It was made up of five layers, with side lobe levels suppressed using a four-corner-fed structure with angled coupling slots. An input aperture, feeding waveguide, and coupling slots made up the feeder. Coburn et al24 used inclined coupling slots to feed four 8 x 8 sub array SWAs with one layer of feeding but four separate feeding [2][3] structures to produce low sidelobe levels for HPM applications. A planar SWA for HPM applications was also presented by Kim et al. Radiating slot plate, radiating waveguide, feeding waveguide, and E-plane septum divider were the four layers of the planar. To manage the feeding to the SWA elements, it was additionally divided into 8 4 sub arrays, each coupled to a multistage divider.

Our project's main goal is to create a 10 * 10 pencil-shaped SWA antenna and determine its gain, power handling, directivity, and efficiency. Slot displacements from the wall centerline are used to determine the antenna's side lobe level (SLL) and to examine the antenna radiation pattern. To find the coefficency and displacement for related ways to compute the frequency range, models based on Taylor and Chebyshev distributions are utilised. A prototype SWA has been simulated and tested, with results that are consistent with the design.

2.1 RELATED WORK

Rashad Hassan [1] et.al. This thesis presents the design and fabrication of a single waveguide resonator-based aperture antenna with a 3rd order band pass filter to demonstrate the concept. The design concept is further improved to merge band pass filters with an aperture antenna array based on NN waveguide resonators. This serves to both boost the array's gain and provide filtering. The antenna array-filter is the integrated component here. Tarek Naous [2] et.al The design of filled SWAs was not optimal for a specific SLR, according to the few studies that looked into it. Based on input specifications of the antenna's SLR, reflection coefficient, frequency of operation, and relative permittivity of the dielectric material, we formulate the design of dielectric-filled SWAs as a regression problem for an accelerated design process in the case of specified SLRs, where the developed ML model predicts the filled SWA's design parameters with very low error. Coburn, William [3] et. al. The array is modular to make fabrication easier and to improve transportability and reparability (with four symmetric modules). The use of a rectangular waveguide corporate-feed network reduces the antenna subsystem volume (i.e., depth), allowing the HPM source to be integrated into the feed structure. An S-band array and feed structure were built and integrated for laboratory testing. The array was manufactured with WR-284 copper waveguide and brass end caps to a 5-mil tolerance. The array's design, fabrication, assembly, and testing are all taken care of. We present preliminary test findings for one of the four modules in the full array. The array's performance will need to be "fine-tuned" after fabrication, as expected.

M. Al-Husseini [4] et.al. The antenna is optimised for 3 GHz operation. The length and width of the slots are optimised for this frequency, and their displacements are calculated with a 20 dB sidelobe level ratio in mind. The azimuth plane beam is then symmetrically focused and increased by adding two rectangular metal sheets as reflectors. Giovanni Andrea Casula [5] et.al. The T-junction feeding the array, the effect of interaction between each slot coupler of the feeding network and the radiating slots closest to this coupler, and the waveguide bends are all under consideration. When compared to the ideal scenario, all of these effects can significantly increase the initial sidelobes, resulting in a significant decrease in array performance.

3. TECHNICAL SPEICIFCATION

1. Antenna Configuration

Because the desired frequency is 3 GHz, the SWA is built using a WR-284 waveguide with a = 2.8400 and b = 1.3700. One end of the waveguide is shorted, while the other is fed. One of its broadsides has ten elliptical grooves carved into it. The slots are separated half the guide wavelength from centre to centre, with the guide wavelength in this case being g = 138.5 mm. The slots are arranged so that the centre of the first, Slot1, is g/4 away from the waveguide feed and the centre of the last, Slot10, is g/4 away from the waveguide's short-circuited side. The waveguide's entire length is thus 5g.

The width of each slot is fixed at 5 mm, which is 2 times the ellipse's minor radius. This is determined as follows: for X-band SWAs, the adopted width of a rectangular slot is 0.062500, equivalent to a = 0.9 00 in the literature. The width of the elliptical slot for this S-band SWA is calculated from 2.8400 0.0625/0.9, which is 0.19700 or 5 mm, using proportionality. The length of the slots (twice the major radius) is projected to be greater than half the free space wavelength due to their elliptical form.

The proposed method for determining the slot displacements from the waveguide axis for a desired SLR is described. The dimensions and guide wavelength of the waveguide utilised in the radiating SWAs are then used to create the feeder SWA. The radiating SWAs are eventually placed side by side, and the feeder is connected to them.

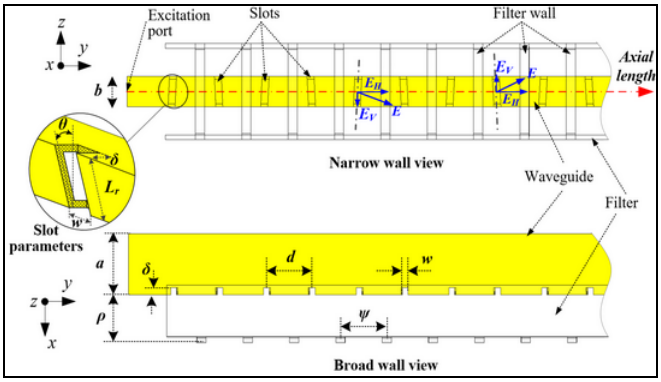

Fig: Panel Design Structure

The three-dimensional SWA arrays in are mirrored in their two-dimensional equivalents in the xz-plane, as illustrated in Figure, allowing for the creation of the proposed antenna while still offering a physical understanding of its geometrical structure. As a result, the proposed case's evolution is presented. The Type A conventional antenna [9] with a wide flare-angle reflector in Figure 5 provides an optimal gain of more than 30 dB at the cost of a huge antenna size. The most straightforward way to shrink the antenna's physical size is to shrink the reflector. Unfortunately, using this method reduces antenna gain significantly.

The slots length can be either nonuniform, in which case the length of each slot is computed using optimization algorithms, or uniform, in which case the length of each

slot is considered to be uniform for simplicity. Choosing uniform slot lengths can also help you achieve your goals.

$$\text{Slot width} = a \times \frac{0.0625\ in}{0.9\ in}.$$

The location of the slots along the length of the SWA is critical for keeping the slots fed in phase. The electrical distance 2d/g2d/g, with gg being the guide wavelength defined as the distance travelled by the electromagnetic wave down the length of the waveguide to suffer a phase shift of 22 radians, determines the phase shift between consecutive slots. (2) is used to determine it, with 00 representing the free-space wavelength and c representing the speed of light..

$$\lambda_g = \frac{\lambda_0}{\sqrt{1-\left(\frac{\lambda_0}{\lambda_{cutoff}}\right)^2}} = \frac{c}{f} \times \frac{1}{\sqrt{1-\left(\frac{c}{2a.f}\right)^2}}.$$

The waveguide operates as a transmission line by using longitudinal slots. The TE10 mode dispersion is symmetrical when a transverse electric field is applied to each slot. Each slot is depicted as a shunt element using an equivalent transmission line. When the width of the slots is narrow[12], their offsets are not too great, and the height of the waveguide is relatively large, this assumption has been proven to be valid using the method of moment.

- • The antenna converts electrical energy from the transmitter into electromagnetic energy, which is then radiated into space; on the receiving end, the antenna converts electromagnetic energy into electrical energy, which is then fed into the receiver: The fundamentals of transmit and receive antenna operation[12]
- • Transmission - sends electromagnetic energy into space
- In two-way communication, the same antenna can be used for transmission and reception, thanks to the high frequency microwave's short wavelength, which allows for the use of highly directional antenna. The use of a microwave antenna for long-distance signal transmission is more cost-effective. The use of a waveguide is ideal for signal transmission across short distances.

4. Metrical Method

Chebyshev Distribution at 20 dB SLR The objective in this case is a 20 dB SLR, and the cns are chosen using a Chebyshev distribution. Slot displacements and coefficients The coefficients cns of a Chebyshev distribution are determined using the following formulae. A generalized Chebyshev array's array factor is written as:

$$f(u) = \prod_{n=1}^{p}\left(\frac{1}{R_n}T_{N_n-1}\left(\gamma_n \cos\frac{u}{2}\right)\right) = \frac{1}{R}\prod_{n=1}^{p}\left(T_{N_n-1}\left(\gamma_n \cos\frac{u}{2}\right)\right)$$

Where:

• Tx signifies a Chebyshev polynomial of order x,

• n = cosh[cosh1(Rn)/(Nn 1)],

• u = 2(d/)(cos cos 0),

• Rn denotes the sidelobe level ratio of the nth basis Chebyshev array, and Nn denotes the number of elements of the nth basis array. The array factor can be stated as: with uniform spacing and a symmetrical amplitude about the centre

$$f(u) = \begin{cases} 2\sum_{m=1}^{N/2} I_m \cos[(m-1/2)u], & \text{for } N \text{ even} \\ \sum_{m=1}^{(N+1)/2} \epsilon_m I_m \cos[(m-1)u], & \text{for } N \text{ odd} \end{cases}$$

Where m equals 1 for m = 1 and equals 2 for m = 1. Finally, the excitation coefficients are found

$$I_m = \begin{cases} \frac{2}{NR}\sum_{q=1}^{N/2} f[u=p]\cos[q], & \text{for } N \text{ even} \\ \frac{1}{NR}\sum_{q=1}^{\frac{N+1}{2}} \epsilon_q f[u=v]\cos[w], & \text{for } N \text{ odd} \end{cases}$$

where:

• p = 2π/N (q − 1/2), • q = 2π/N (m − 1/2) (q − 1/2),

• v = 2π/N (q − 1), • and w = 2π/N (m − 1) (q − 1).

Table: Slot displacements in radiating and feeder SWAs for the 8 × 8 planar SWA example

	Displacement (mm)	
Slot number	SWA branchlines (WR-229)	SWA feeder (WR-187)
1 & 8	2.78	1.88
2 & 7	4.36	2.94
3 & 6	5.71	3.85
4 & 5	6.48	4.36

First, the Feeder SWA and the eight radiating SWAs are made. The slots were drilled with a 3 mm type carbide on a HAAS VF-6 three axis milling machine with an accuracy of 0.001 mm.

Coefficients and Slots Displacements

The following formulae can be used to calculate the c_ns for a Taylor one-parameter distribution. For a continuous line distribution of length l, the excitation coefficients, In(z), are equal to

$$I_n(z') = \begin{cases} J_0\left[j\pi B\sqrt{1-\left(\frac{2z'}{l}\right)^2}\right], & \text{for } -l/2 \leqslant z' \leqslant +l/2, \\ 0, & \text{elsewhere} \end{cases}$$

The current magnitudes of an N-element linear array with symmetric excitation are equivalent as in the discrete case [12]

$$a_m = \begin{cases} I_0\left[\beta\sqrt{1-\left(\frac{m-0.5}{M-0.5}\right)^2}\right], & \text{for } N = 2M \\ I_0\left[\beta\sqrt{1-\left(\frac{m-1}{M-1}\right)^2}\right], & \text{for } N = 2M-1 \end{cases}$$

A 30 dB Taylor (one-parameter) taper is necessary for a 20 dB SLL for the SWA. The derived coefficients, as well as the slot displacements.

Table –SWA SLL of 20 dB due to 30 dB Taylor (one-parameter) coefficients and related slots displacements.

Slot Number	Chebyshev Coefficient GhZ	Displacement (mm)
1	1	3.74
2	2.086	5.42
3	3.552	7.11
4	4.896	8.4
5	5.707	9.11
6	5.707	9.11
7	4.896	8.4
8	3.552	7.11
9	2.086	5.42
10	1	3.74

A Taylor (one-parameter) distribution is utilised in this example to generate a SWA SLR of 30 dB. The taper coefficients for a 40 dB Taylor (one-parameter) distribution are needed for this, and they're listed in Table 3 with their corresponding slots displacements. The results demonstrate a 3 GHz antenna resonance with a 15.3 dB peak gain.

Table 3 lists the binomial coefficients and corresponding slots displacements for the case of ten slots. The obtained SLR is 33.5 dB, and the max gain is 15 dB for these displacement values. The HPBW in the Y Z-plane rises to 11.1 degrees.

Table: Coefficients and corresponding slots displacements

Slot Number	Taylor-based Coefficient	Displacement (mm)
1	1	3.493
2	2.467	5.518
3	4.137	7.194
4	5.597	8.419
5	6.449	9.070
6	6.449	9.070
7	5.597	8.419
8	4.137	7.137
9	2.467	5.518
10	1	3.493

Measurement

A prototype SWA array was constructed and tested to confirm the procedure presented. The waveguide in my hand is 50 cm long. Because this length is insufficient to accommodate 10 slots while adhering to the various slot distance and length criteria, the design was modified to include 7 elliptical slots. The distance between each of these two edge slots and the adjoining waveguide edge has been raised from g/4 to 3g/4 to avoid the two edge slots intersecting the waveguide flanges, resulting in a total SWA length of 4.5g. The Python computer software that was utilised for this design allowed for this modification. The SWA is built for a frequency of 50 kHz to maintain the waveguide length of 50 cm. , 4.5g = 50 cm, and g = 111.11 mm. The elliptical slot length has been tuned to attain to this resonance frequency after the SWA was designed with the correct uniform distribution displacement. It is discovered to be 48 mm. The SWA was later built to radiate with a sidelobe level of less than 20

dB using this optimised length and a slot width of 5 mm. In this case, the excitation coefficients were calculated using a Chebyshev distribution of 35 dB. lists these coefficients as well as the related slot displacements.

The antenna design and a shot of the prototype may be found here. The reflection coefficient plot provides a comparison of two measured data and simulated results computed using both CST and HFSS software. The antenna had some protrusions on the corners of the elliptical slots during Measurement 1, which were filed for Measurement 2, giving the slot a perfect elliptical form. In comparison to the measured data, the gain patterns estimated in both HFSS and CST are. Despite the tiny variation, which is attributable to other fabrication flaws, a credible parallel has been shown by inspecting the S11 and pattern figures.

5. EXPERIMENTAL RESULTS

The patch antenna is made up of three bricks: one for the radiating plate, one for the microstrip line, and one for the substrate, which uses CST and HFSS. A completely electrically conducting boundary condition defines the ground plane. Assigning coordinates is done as follows. The ground plane and substrate begin at this point (0,0,0). The substrate's length, L, and breadth, W, are chosen to be 28.1 mm and 32 mm, respectively. The patch's length is 0/2 12.45 mm, and its breadth is half that of the ground, with a substrate of 16 mm. The patches, on the other hand, begin at (28.1/4, 32/4, 0).The patch's beginning point is 14 percent of the ground plane's overall width, and it stretches 12.45 mm in the positive x-direction. Similarly, the patch is 14 of the total length of the ground plane in the x-y plane (z=0) in the y-direction. Furthermore, the feed line should be situated between the patch's starting point and finishing point values.

Fig: SWA Design Calculation

Select File > Save As from the File menu in the Ansoft HFSS window. Type the desired file name in the Save As window. Select the Save button. This is how your final model should look:

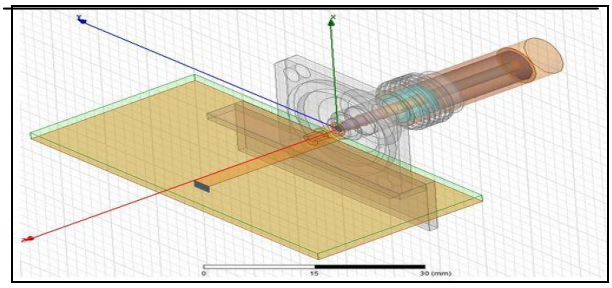

Fig: SWA Antenna

A slot antenna is made up of a metal surface having a hole or slot carved out of it, commonly a flat plate. When a driving frequency is used to drive the plate as an antenna, the slot radiates electromagnetic waves in the same way that a dipole antenna does. The radiation distribution pattern is determined by the form and size of the slot, as well as the driving frequency. The slots on the waveguide will be assumed to have a narrow width. Increased width increases bandwidth (remember that a fatter antenna frequently has more bandwidth); nevertheless, a wider width comes at the cost of increased cross-polarization. Fractional Bandwidth (FBW) for thin slots can be as low as 3-5 percent, whereas FBW for large slots can be as high as 75 percent. Figure shows an example of a slotted waveguide array (dimensions supplied by length a and width b) slot waveguide with dimensions given by length a and width b.

Table: Microstrip Line

Starting Point (mm)	Full Length (mm)
x = 7.025	dx = 12.45
y = 8	dy = 16
z = 0	dz = 0.05

it would now be simple to draw the model. You only need to enter in the coordinates. Let's begin by sketching the ground plane. Please refer to Table 3 for Ground Plane coordinates. Choose Draw> Box from the menu. Enter the box position (x, y, z) in the coordinate entry fields in Table 3, then the opposite corner of the base rectangle (dx, dy, dz), where dx, dy, and dz stand for full length, full width, and full height, respectively. The ground plane's dimensions are given. When the properties dialogue box displays, double-check that the Position, Xsize, Ysize, and Zsize values are correct.

Select the Attribute tab and type gnd as the name's value. Assign PEC (Perfect Electric Conductor) material to the object by clicking on it. Then select your preferred colour and transparency value. Select the OK option.

Let's draw the substrate next. The substrate and the ground plane have the same dimensions. Because the ground plane is at z = -0.794 and has no thickness (dz=0), the substrate must be 0.794 mm thick, and since the beginning point was zero, the complete height must be in the -z direction. Draw > Box with the coordinates from Table 4, set the box's location (x, y, z), and enter the box's opposite corner (dx, dy, dz).

Coordinates are correct. Enter Substrate in the name value box on the Attribute tab. Assign Rogers RT/Duroid 5880(tm) with a relative permittivity of 2.2 to the material. Click OK. Select your preferred colour and transparency value once again. Select the OK option.

Finally, make the patch. Knowing that the patch should be in the middle, calculating the coordinates from the ground and substrate dimensions is simple. The patch's centre, ground plane, and substrate are all the same size and are located at (28.1/2, 32/2, 0). To calculate the starting point, subtract the centre point coordinates from the substrate coordinates, and the patch's complete length, width, and height are given. Draw > Box, your coordinates are correct. Under the name value box, type Patch in the Attribute tab. Assign PEC to the stuff now. Click OK. Select your preferred colour and transparency value once again..

RESULT AND DISCUSSION

Performance Analysis

A few characteristics, including as return loss, bandwidth, radiation pattern, directivity, and antenna gain, determine the performance of a designed antenna.

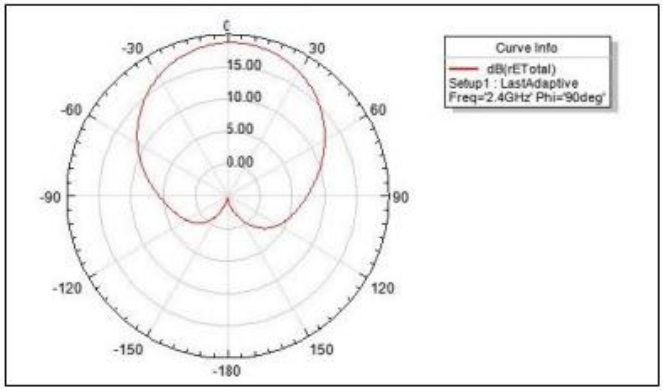

Fig: 2.4 GHz frequency radiation pattern.

It shows the antenna gain when phi is 90 degrees. An antenna's gain is defined as the ratio of intensity in one direction to the radiation intensity that would be obtained if the antenna's power was emitted in an isotropic way. The antenna's gain is proportional to its directivity. An antenna's gain refers to its efficiency as well as its directional capabilities. Gives the relationship between an antenna's gain and directivity.

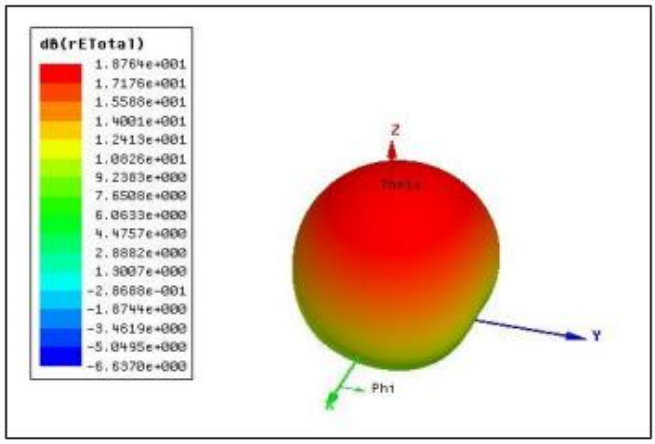

Fig: Radiation pattern in three dimensions at 2.4 GHz

In terms of SS11, far-fields E-plane and H-plane, and gain, modelling results for the proposed array antenna 10 *10 are displayed. The array antenna's simulated resonance frequency is 2.4 GGGGGG, with a reflection coefficient of around 34.36 dddd. This array antenna's simulated impedance bandwidth is around 30 MHz (2.38-2.41 GHz). The array antenna 10 *10's simulated two-dimensional far-fields E-plane and H-plane at 2.4 GHz. It's worth noting that the proposed array antenna 10*10 has a very directed emission pattern in both planes E and H. The array antenna has also been shown to have a very high gain of roughly 10.22 dB. Table 3 compares the performance of the proposed array antenna with that of other array antennas for RFID systems. The proposed array antenna has a modest and acceptable size and a substantially higher gain than existing reference works, as shown in the Table.

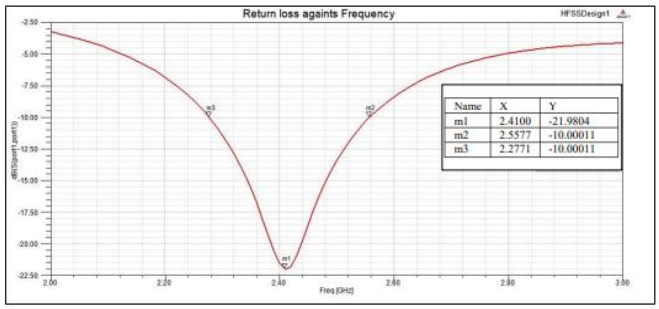

Fig: Return loss versus. frequency for a patch antenna operating at 2.4 GHz

Because of mismatches between the transmission line and the feeding points, the return loss shows how much feeding power was reflected back at the patch antenna's port. Reflections at the antenna port move back towards the source when the antenna and transmission line are not exactly matched, forming a standing wave. High return loss is required for a good antenna. The antenna radiates best at the chosen resonance frequency, 2.4 GHz, with a return loss of 20 dB, according to from.

Bandwidth

The bandwidth of an antenna refers to the frequency range over which it can function properly. The antenna's bandwidth is defined as the number of Hz for which the SLR is less than 2. The graph return loss against frequency at point 10 dB[11] can be used to determine the bandwidth value. The value of bandwidth is 0.28 dB, as demonstrated in the graph of return loss against frequency. The bandwidth restriction of various antenna types varies.

It indicates how much power is reflected back to the source from the antenna. The acceptable value for an antenna is 1 VSWR 2. If the VSWR value is 1, the antenna receives all of the power it is provided. Figure 6 shows theFrom figure 6, the value for designed antenna is 1.

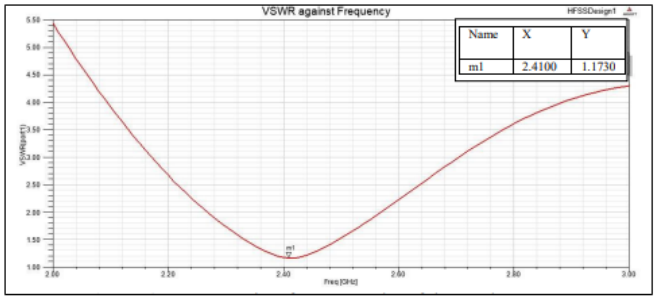

Fig: frequency plot of the patch antenna.

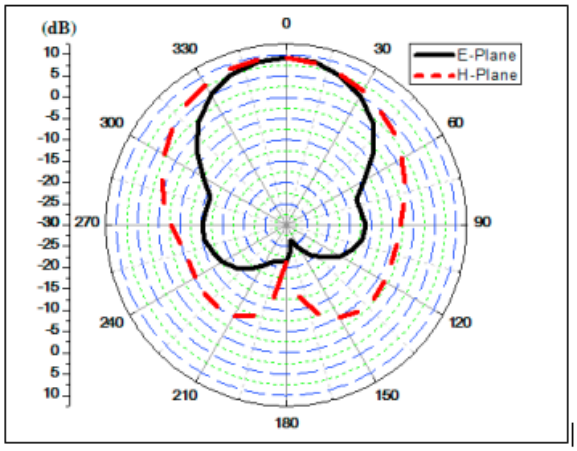

Fig: Simulated E and H planes at 2.40 GHz

The prototype antennas' design and a shot of the prototype. The reflection coefficient plot compares two measured results with simulated results computed using both CST and HFSS software.

CST was used to replicate the planned planar SWA. Table 2 lists the computed SLR, HPBW, and gain in the E- and H-planes, with a 3D gain pattern plot in Figure 5. As can be seen, a pencil form pattern was achieved with an SLR of not less than 20 dB in both planes, narrow HPBW, and is suited for HPM applications. If the required SLR utilised to detect the slots displacements is made larger than 20 dB, lower sidelobe levels are easily obtained.

Table: 10*10 SWA Antenna Simulation Results

ANTENNA	E- PLANE		H-PLANE		GAIN
TYPE	SLR	HPBW	SLR	HPBW	(dB)
10*10 SWA	24.7 dB	10	27.3dB	12.5"	33.75

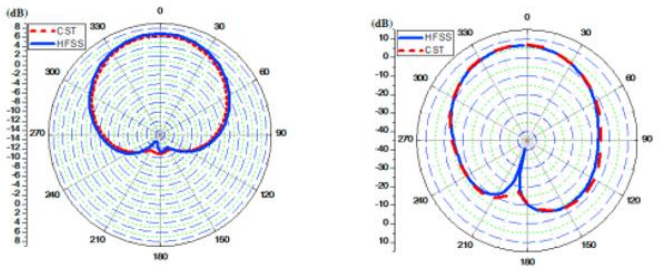

Fig: A) E-plane radiation pattern simulation (B) element patch antenna at 2.4 GHz

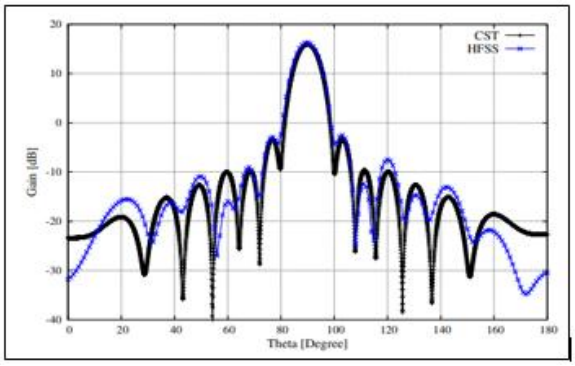

Fig: For the scenario of non-uniform slots displacements with Chebychev distribution, the antenna's Y Z-plane pattern for 20dB

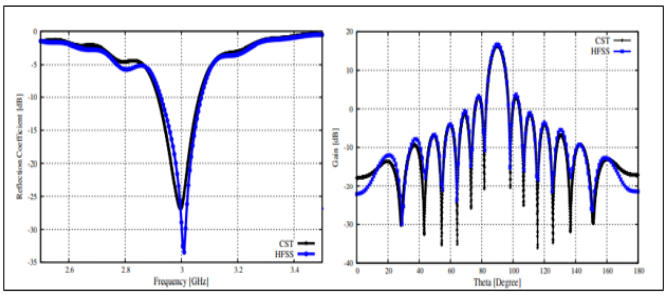

Fig: The findings of the measured and simulated reflection coefficients were compared.

The feeder SWA is then welded to the radiating SWAs utilising the back of the radiating SWAs' L-shaped copper corners. Figure 6 depicts the manufactured planar SWA. In Figure 7, the simulated gain pattern results are compared to the measured ones. The findings of the measured reflection coefficient are also shown.

Figure 8 shows the results of simulations using CST. As can be observed, the measured results are extremely similar to the simulated ones, and they are also consistent with the design goals. This antenna array's capacity to break down has also been investigated. On the slot responsible for the most radiation, the maximum voltage value has been computed. The slots in the centre of the array system give the most radiation because they have the highest fed power intake from the SWA feeder and the greatest displacements from the SWA branch line centerline where the slots are located.. The maximum voltage on these slots is found to be 5.55 105 V/m when the system is simulated with a high input power to the feeder SWA of 6.25 MW. This maximum voltage is still lower than the commencement of air breakdown, which can cause the air to begin to break down at 3 106 V/m. If desired, a bigger slot width value can be used to provide a lower maximum voltage and hence a higher value of power radiated.

6. CONCLUSION

The performance parameters of the developed SWA in this research work are shown utilizing the basic antenna parameter characteristics of resonant frequency, return loss (S11), VSWR, Bandwidth, Gain, Directivity, Half Power Beam width (HPBW), and Efficiency..

REFERENCES:

1. Rueggeberg W. A multislotted waveguide antenna for high-powered microwave heating systems. IEEE Trans Ind Appl. 1980;6:809-813.

2. Gilbert RA, Volakis JL. Waveguide slot antenna arrays. Antenna Eng Handbook. 2007;9:14.

3. Mailloux RJ. Phased Array Antenna Handbook. Massachusetts: Artech house; 2017.

4. Lo YT, Lee SW. Antenna Handbook: Theory, Applications, and Design. Germany: Springer Science & Business Media; 2013.

5. Elliott R, Kurtz L. The design of small slot arrays. IEEE Trans Antennas Propag. 1978;26(2):214-219.

6. Elliott R. On the design of traveling-wave-fed longitudinal shunt slot arrays. IEEE Trans Antennas Propag. 1979;27(5):717-720.

7. Stevenson AF. Theory of slots in rectangular wave-guides. J Appl Phys. 1948;19(1):24-38.

8. Elliott RS. An improved design procedure for small arrays of shunt slots. IEEE Trans Antennas Propag. 1983;31(1):48-53.

9. Stegen RJ. Longitudinal shunt slot characteristics. Hughes aircraft co culver city ca research and development div. Tucson, Arizona: Hughes

Aircraft Co Culver City Ca Research and Development Div; 1951.

10. Tai CT. Characteristics of linear antenna elements. Antenna Engineering Handbook. Pennsylvania, NY: McGraw-Hill; 1961:3-8.

11. Oliner A. The impedance properties of narrow radiating slots in the broad face of rectangular waveguide: Part I–theory.IRE Trans Antennas

Propag. 1957;5(1):4-11.

12. Pan X, Christodoulou CG. A narrow-wall slotted waveguide antenna array for high power applications. Paper presented at: Proceedings

of the 2014 IEEE Antennas and Propagation Society International Symposium (APSURSI); 2014:1493-1494; Memphis, TN: IEEE.

13. Pan Xuyuan. A Narrow-wall Complementary-split-ring Slotted Waveguide Antenna for High-power-microwave Applications. Mexico:

Dissertation, Digital Repository, the University of New Mexico; 2018. https://digitalrepository.unm.edu/ece_etds/444.

14. Sabri MW, Murad NA, Rahim MKA. Highly directive 3D-printed dual-beam waveguide slotted antennas for millimeter-wave applications. Microw Opt Technol Lett. 2019;61(6):1566-1573.

15. Pulido-Mancera LM, Zvolensky T, Imani MF, Bowen PT, Valayil M, Smith DR. Discrete dipole approximation applied to highly directive slotted waveguide antennas. IEEE Antennas Wirel Propag Lett. 2016;15:1823-1826.

16. Costa IF, Cerqueira S Arismar, SDH. Dual-band slotted waveguide antenna array for adaptive mm-wave 5G networks. Paper presented at: Proceedings of the 2017 11th European Conference on Antennas and Propagation; 2017:1322-1325; Paris, France: IEEE.

17. Filgueiras HRD, Costa IF, Cerqueira A, Kelly JR, Xiao P. A novel approach for designing omnidirectional slotted-waveguide antenna arrays. Paper presented at: Proceedings of the 2018 International Conference on Electromagnetics in Advanced Applications (ICEAA 2018); 2018:64-67; Cartagena des Indias, Colombia: IEEE.

18. Tan L, Zhang J, Wang W, Xu J. Design of a W-band one-dimensional beam scanning slotted waveguide antenna with narrow beam and low side lobe. Paper presented at: Proceedings of the 2017 Progress in Electromagnetics Research Symposium-Spring; 2017:3625-3628; St. Petersburg, Russia: IEEE.

19. Le Sage GP. 3D printed waveguide slot array antennas. IEEE Access. 2016;4:1258-1265.

20. El Misilmani HM, Al-Husseini M, Kabalan KY. Simple design procedure for 2D SWAs with specified sidelobe levels and inclined coupling slots. 4th Advanced Electromagnetic Symposium (AES 2016), Spain; 2016.